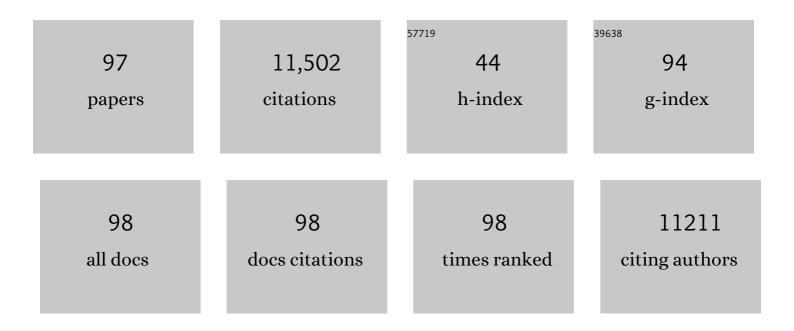
## Liming Zhou

List of Publications by Year in descending order

Source: https://exaly.com/author-pdf/5750204/publications.pdf Version: 2024-02-01



LIMING 7HOLL

#	Article	IF	CITATIONS
1	Weather, Climatic and Ecological Impacts of Onshore Wind Farms. , 2022, , 165-188.		О
2	The most extreme heat waves in Amazonia happened under extreme dryness. Climate Dynamics, 2022, 59, 281-295.	1.7	6
3	Recent rainfall conditions in the Congo Basin. Environmental Research Letters, 2022, 17, 054052.	2.2	1
4	Orographic enhancement of rainfall over the Congo Basin. Atmospheric Science Letters, 2022, 23, .	0.8	2
5	Moisture transport and water vapour budget over the Sahara Desert. International Journal of Climatology, 2022, 42, 6829-6843.	1.5	2
6	Relationships between intense convection, lightning, and rainfall over the interior Congo Basin using TRMM data. Atmospheric Research, 2022, 273, 106164.	1.8	2
7	Evaporative water loss of 1.42 million global lakes. Nature Communications, 2022, 13, .	5.8	49
8	Analyzing intensifying thunderstorms over the Congo Basin using the GÃilvez-Davison index from 1983–2018. Climate Dynamics, 2021, 56, 949-967.	1.7	8
9	Increasing Influence of Indian Ocean Dipole on Precipitation Over Central Equatorial Africa. Geophysical Research Letters, 2021, 48, e2020GL092370.	1.5	11
10	Rising Planetary Boundary Layer Height over the Sahara Desert and Arabian Peninsula in a Warming Climate. Journal of Climate, 2021, 34, 4043-4068.	1.2	12
11	Reconciling Human and Natural Drivers of the Tripole Pattern of Multidecadal Summer Temperature Variations Over Eurasia. Geophysical Research Letters, 2021, 48, e2021GL093971.	1.5	10
12	Vegetation Greening Offsets Urbanizationâ€Induced Fast Warming in Guangdong, Hong Kong, and Macao Region (GHMR). Geophysical Research Letters, 2021, 48, e2021GL095217.	1.5	11
13	A shift in the diurnal timing and intensity of deep convection over the Congo Basin during the past 40Âyears. Atmospheric Research, 2021, 264, 105869.	1.8	4
14	Diurnal asymmetry of desert amplification and its possible connections to planetary boundary layer height: a case study for the Arabian Peninsula. Climate Dynamics, 2021, 56, 3131-3156.	1.7	11
15	High-Resolution WRF Simulation of Extreme Heat Events in Eastern China: Large Sensitivity to Land Surface Schemes. Frontiers in Earth Science, 2021, 9, .	0.8	6
16	The MJO's impact on rainfall trends over the Congo rainforest. Climate Dynamics, 2020, 54, 2683-2695.	1.7	12
17	Observed changes in fire patterns and possible drivers over Central Africa. Environmental Research Letters, 2020, 15, 0940b8.	2.2	18
18	Effects of Nonuniform Land Surface Warming on Summer Anomalous Extratropical Cyclone Activity and the East Asian Summer Monsoon: Numerical Experiments with a Regional Climate Model. Journal of Climate, 2020, 33, 10469-10488.	1.2	8

#	Article	IF	CITATIONS
19	Analyzing Meteorological and Chemical Conditions for Two High Ozone Events Over the New York City and Long Island Region. , 2020, , .		0
20	Widespread increase of boreal summer dry season length over the Congo rainforest. Nature Climate Change, 2019, 9, 617-622.	8.1	70
21	Impacts of increased urbanization on surface temperature, vegetation, and aerosols over Bengaluru, India. Remote Sensing Applications: Society and Environment, 2019, 16, 100261.	0.8	23
22	Validation of Satellite Precipitation Estimates over the Congo Basin. Journal of Hydrometeorology, 2019, 20, 631-656.	0.7	49
23	Simulating impacts of real-world wind farms on land surface temperature using the WRF model: physical mechanisms. Climate Dynamics, 2019, 53, 1723-1739.	1.7	26
24	Trends in Tropical Wave Activity from the 1980s to 2016. Journal of Climate, 2019, 32, 1661-1676.	1.2	19
25	Assessing reanalysis data for understanding rainfall climatology and variability over Central Equatorial Africa. Climate Dynamics, 2019, 53, 651-669.	1.7	61
26	An Externally Forced Decadal Rainfall Seesaw Pattern Over the Sahel and Southeast Amazon. Geophysical Research Letters, 2019, 46, 923-932.	1.5	31
27	Understanding the Central Equatorial African long-term drought using AMIP-type simulations. Climate Dynamics, 2018, 50, 1115-1128.	1.7	44
28	Changing response of the North Atlantic/European winter climate to the 11 year solar cycle. Environmental Research Letters, 2018, 13, 034007.	2.2	20
29	Increasing extent and intensity of thunderstorms observed over the Congo Basin from 1982 to 2016. Atmospheric Research, 2018, 213, 17-26.	1.8	34
30	Divergent hydrological response to large-scale afforestation and vegetation greening in China. Science Advances, 2018, 4, eaar4182.	4.7	287
31	New Rainfall Datasets for the Congo Basin and Surrounding Regions. Journal of Hydrometeorology, 2018, 19, 1379-1396.	0.7	28
32	Land–atmosphere–aerosol coupling in North China during 2000–2013. International Journal of Climatology, 2017, 37, 1297-1306.	1.5	8
33	Observational Evidence for Desert Amplification Using Multiple Satellite Datasets. Scientific Reports, 2017, 7, 2043.	1.6	17
34	Climate mitigation from vegetation biophysical feedbacks during the past three decades. Nature Climate Change, 2017, 7, 432-436.	8.1	323
35	Simulating Impacts of Real-World Wind Farms on Land Surface Temperature Using the WRF Model: Validation with Observations. Monthly Weather Review, 2017, 145, 4813-4836.	0.5	26
36	Evaluation of simulated climatological diurnal temperature range in CMIP5 models from the perspective of planetary boundary layer turbulent mixing. Climate Dynamics, 2017, 49, 1-22.	1.7	52

#	Article	IF	CITATIONS
37	Observational Quantification of Climatic and Human Influences on Vegetation Greening in China. Remote Sensing, 2017, 9, 425.	1.8	81
38	Satellite Observations of El Niño Impacts on Eurasian Spring Vegetation Greenness during the Period 1982–2015. Remote Sensing, 2017, 9, 628.	1.8	24
39	Detecting Wind Farm Impacts on Local Vegetation Growth in Texas and Illinois Using MODIS Vegetation Greenness Measurements. Remote Sensing, 2017, 9, 698.	1.8	20
40	Possible causes of the Central Equatorial African long-term drought. Environmental Research Letters, 2016, 11, 124002.	2.2	100
41	Desert Amplification in a Warming Climate. Scientific Reports, 2016, 6, 31065.	1.6	36
42	A case study of effects of atmospheric boundary layer turbulence, wind speed, and stability on wind farm induced temperature changes using observations from a field campaign. Climate Dynamics, 2016, 46, 2179-2196.	1.7	46
43	Mechanisms for stronger warming over drier ecoregions observed since 1979. Climate Dynamics, 2016, 47, 2955-2974.	1.7	40
44	Assessing climatic impacts of future land use and land cover change projected with the CanESM2 model. International Journal of Climatology, 2015, 35, 3661-3675.	1.5	34
45	Stronger warming amplification over drier ecoregions observed since 1979. Environmental Research Letters, 2015, 10, 064012.	2.2	60
46	Observed Thermal Impacts of Wind Farms Over Northern Illinois. Sensors, 2015, 15, 14981-15005.	2.1	29
47	China experiencing the recent warming hiatus. Geophysical Research Letters, 2015, 42, 889-898.	1.5	111
48	Satellite-indicated long-term vegetation changes and their drivers on the Mongolian Plateau. Landscape Ecology, 2015, 30, 1599-1611.	1.9	88
49	Evaporative cooling over the Tibetan Plateau induced by vegetation growth. Proceedings of the National Academy of Sciences of the United States of America, 2015, 112, 9299-9304.	3.3	404
50	Regional air pollution brightening reverses the greenhouse gases induced warmingâ€elevation relationship. Geophysical Research Letters, 2015, 42, 4563-4572.	1.5	30
51	Sunlight mediated seasonality in canopy structure and photosynthetic activity of Amazonian rainforests. Environmental Research Letters, 2015, 10, 064014.	2.2	90
52	Satellite Observations of Wind Farm Impacts on Nocturnal Land Surface Temperature in Iowa. Remote Sensing, 2014, 6, 12234-12246.	1.8	46
53	A 3D Canopy Radiative Transfer Model for Global Climate Modeling: Description, Validation, and Application. Journal of Climate, 2014, 27, 1168-1192.	1.2	49
54	Impact of precipitationâ€induced sensible heat on the simulation of landâ€surface air temperature. Journal of Advances in Modeling Earth Systems, 2014, 6, 1311-1320.	1.3	19

#	Article	IF	CITATIONS
55	Afforestation in China cools local land surface temperature. Proceedings of the National Academy of Sciences of the United States of America, 2014, 111, 2915-2919.	3.3	501
56	Detection of urbanization signals in extreme winter minimum temperature changes over Northern China. Climatic Change, 2014, 122, 595-608.	1.7	29
57	Widespread decline of Congo rainforest greenness in the past decade. Nature, 2014, 509, 86-90.	13.7	351
58	Diurnal and seasonal variations of wind farm impacts on land surface temperature over western Texas. Climate Dynamics, 2013, 41, 307-326.	1.7	48
59	Hotspots of the sensitivity of the land surface hydrological cycle to climate change. Science Bulletin, 2013, 58, 3682-3688.	1.7	16
60	Spatiotemporal Structure of Wind Farm-atmospheric Boundary Layer Interactions. Energy Procedia, 2013, 40, 530-536.	1.8	25
61	Effects of Topography on Assessing Wind Farm Impacts Using MODIS Data. Earth Interactions, 2013, 17, 1-18.	0.7	19
62	Change in snow phenology and its potential feedback to temperature in the Northern Hemisphere over the last three decades. Environmental Research Letters, 2013, 8, 014008.	2.2	125
63	Response to Comment on "Surface Urban Heat Island Across 419 Global Big Citiesâ€: Environmental Science & Technology, 2012, 46, 6889-6890.	4.6	15
64	Surface Urban Heat Island Across 419 Global Big Cities. Environmental Science & Technology, 2012, 46, 696-703.	4.6	864
65	Impacts of wind farms on land surface temperature. Nature Climate Change, 2012, 2, 539-543.	8.1	228
66	Sensitivity of simulated terrestrial carbon assimilation and canopy transpiration to different stomatal conductance and carbon assimilation schemes. Climate Dynamics, 2011, 36, 1037-1054.	1.7	33
67	Changes in cloudiness over the Amazon rainforests during the last two decades: diagnostic and potential causes. Climate Dynamics, 2011, 37, 1151-1164.	1.7	32
68	Detection and attribution of anthropogenic forcing to diurnal temperature range changes from 1950 to 1999: comparing multi-model simulations with observations. Climate Dynamics, 2010, 35, 1289-1307.	1.7	84
69	Spatial dependence of diurnal temperature range trends on precipitation from 1950 to 2004. Climate Dynamics, 2009, 32, 429-440.	1.7	139
70	Spatiotemporal patterns of changes in maximum and minimum temperatures in multiâ€model simulations. Geophysical Research Letters, 2009, 36, .	1.5	45
71	Asymmetric response of maximum and minimum temperatures to soil emissivity change over the Northern African Sahel in a GCM. Geophysical Research Letters, 2008, 35, .	1.5	18
72	Dynamics of leaf area for climate and weather models. Journal of Geophysical Research, 2008, 113, .	3.3	14

#	Article	IF	CITATIONS
73	A threeâ€dimensional analytic model for the scattering of a spherical bush. Journal of Geophysical Research, 2008, 113, .	3.3	19
74	Impact of Vegetation Types on Surface Temperature Change. Journal of Applied Meteorology and Climatology, 2008, 47, 411-424.	0.6	48
75	Empirical Evidence for Impacts of Internal Migration on Vegetation Dynamics in China from 1982 to 2000. Sensors, 2008, 8, 5069-5080.	2.1	13
76	Climate Response to Rapid Urban Growth: Evidence of a Human-Induced Precipitation Deficit. Journal of Climate, 2007, 20, 2299-2306.	1.2	300
77	Impact of vegetation removal and soil aridation on diurnal temperature range in a semiarid region: Application to the Sahel. Proceedings of the National Academy of Sciences of the United States of America, 2007, 104, 17937-17942.	3.3	151
78	Changes in biomass carbon stocks in China's grasslands between 1982 and 1999. Global Biogeochemical Cycles, 2007, 21, n/a-n/a.	1.9	127
79	Four-stream isosector approximation for canopy radiative transfer. Journal of Geophysical Research, 2007, 112, .	3.3	6
80	Effect of climate and CO2changes on the greening of the Northern Hemisphere over the past two decades. Geophysical Research Letters, 2006, 33, .	1.5	207
81	Variations in satellite-derived phenology in China's temperate vegetation. Global Change Biology, 2006, 12, 672-685.	4.2	643
82	Changes in vegetation net primary productivity from 1982 to 1999 in China. Global Biogeochemical Cycles, 2005, 19, n/a-n/a.	1.9	244
83	Precipitation patterns alter growth of temperate vegetation. Geophysical Research Letters, 2005, 32, .	1.5	179
84	Observational evidence of sensitivity of surface climate changes to land types and urbanization. Geophysical Research Letters, 2005, 32, n/a-n/a.	1.5	112
85	Derivation of a soil albedo dataset from MODIS using principal component analysis: Northern Africa and the Arabian Peninsula. Geophysical Research Letters, 2005, 32, .	1.5	6
86	Evidence for a significant urbanization effect on climate in China. Proceedings of the National Academy of Sciences of the United States of America, 2004, 101, 9540-9544.	3.3	709
87	Remote sensing of vegetation and land-cover change in Arctic Tundra Ecosystems. Remote Sensing of Environment, 2004, 89, 281-308.	4.6	522
88	Interannual variations of monthly and seasonal normalized difference vegetation index (NDVI) in China from 1982 to 1999. Journal of Geophysical Research, 2003, 108, .	3.3	401
89	Increasing net primary production in China from 1982 to 1999. Frontiers in Ecology and the Environment, 2003, 1, 293-297.	1.9	195
90	Analysis of a multiyear global vegetation leaf area index data set. Journal of Geophysical Research, 2002, 107, ACL 14-1.	3.3	85

#	Article	IF	CITATIONS
91	Analysis of interannual changes in northern vegetation activity observed in AVHRR data from 1981 to 1994. IEEE Transactions on Geoscience and Remote Sensing, 2002, 40, 115-130.	2.7	122
92	Multiscale analysis and validation of the MODIS LAI productII. Sampling strategy. Remote Sensing of Environment, 2002, 83, 431-441.	4.6	89
93	Multiscale analysis and validation of the MODIS LAI productl. Uncertainty assessment. Remote Sensing of Environment, 2002, 83, 414-430.	4.6	174
94	Variations in northern vegetation activity inferred from satellite data of vegetation index during 1981 to 1999. Journal of Geophysical Research, 2001, 106, 20069-20083.	3.3	1,244
95	A large carbon sink in the woody biomass of Northern forests. Proceedings of the National Academy of Sciences of the United States of America, 2001, 98, 14784-14789.	3.3	568
96	Effect of orbital drift and sensor changes on the time series of AVHRR vegetation index data. IEEE Transactions on Geoscience and Remote Sensing, 2000, 38, 2584-2597.	2.7	151
97	Spatial-temporal trend of seasonally-integrated normalized difference vegetation index as an indicator of changes in Arctic tundra vegetation in the early 1990s. , 0, , .		1